



**HAL**  
open science

## High Sensitivity CW-Cavity Ring Down Spectroscopy of $^{12}\text{CO}_2$ near $1.35 \mu\text{m}$ (II): New observations and Line intensities modeling

K.F. Song, Samir Kassi, S.A. Tashkun, V.I. Perevalov, Alain Campargue

► **To cite this version:**

K.F. Song, Samir Kassi, S.A. Tashkun, V.I. Perevalov, Alain Campargue. High Sensitivity CW-Cavity Ring Down Spectroscopy of  $^{12}\text{CO}_2$  near  $1.35 \mu\text{m}$  (II): New observations and Line intensities modeling. *Journal of Quantitative Spectroscopy and Radiative Transfer*, 2010, 111, pp.332-344. 10.1016/j.jqsrt.2009.09.004 . hal-00563185

**HAL Id: hal-00563185**

**<https://hal.science/hal-00563185>**

Submitted on 4 Feb 2011

**HAL** is a multi-disciplinary open access archive for the deposit and dissemination of scientific research documents, whether they are published or not. The documents may come from teaching and research institutions in France or abroad, or from public or private research centers.

L'archive ouverte pluridisciplinaire **HAL**, est destinée au dépôt et à la diffusion de documents scientifiques de niveau recherche, publiés ou non, émanant des établissements d'enseignement et de recherche français ou étrangers, des laboratoires publics ou privés.

# High Sensitivity CW-Cavity Ring Down Spectroscopy of $^{12}\text{CO}_2$ near 1.35 $\mu\text{m}$ (II): New observations and Line intensities modeling

K. F. Song <sup>a,b</sup>, S. Kassi <sup>a</sup>, S.A. Tashkun <sup>c</sup>, V. I. Perevalov <sup>c</sup> and A. Campargue <sup>a1</sup>

(a) *Laboratoire de Spectrométrie Physique, UMR CNRS 5588, Université Joseph Fourier, BP 87, 38402 Saint Martin d'Hères Cedex, France*

(b) *Hefei National Laboratory for Physical Sciences at Microscale, Department of Chemical Physics, University of Science and Technology of China, Hefei, 230026, China*

(c) *Laboratory of Theoretical Spectroscopy, Institute of Atmospheric Optics SB RAS, 1 Akademicheskii Avenue, 634055 Tomsk, Russia*

Version: 4 June 2009

Number of tables: 4

Number of figures: 6

\* Corresponding author: [Alain.Campargue@ujf-grenoble.fr](mailto:Alain.Campargue@ujf-grenoble.fr)

Running head: *CO<sub>2</sub> line intensities near 1.35  $\mu\text{m}$ .*

**Key words:** Carbon dioxide, CO<sub>2</sub>, Cavity Ring Down Spectroscopy, line intensities, Global modelling, HITRAN, HITEMP, CDSD, Venus

---

<sup>1</sup> Corresponding author: [Alain.Campargue@ujf-grenoble.fr](mailto:Alain.Campargue@ujf-grenoble.fr)

## Abstract

In a [previous](#) contribution (Kassi S, Song KF, Campargue A. High sensitivity CW-cavity ring down spectroscopy of  $^{12}\text{CO}_2$  near  $1.35\mu\text{m}$  (I): Line positions. *JQSRT* [110](#) (2009) [1801-1814](#)), the line positions analysis of the high sensitivity absorption spectrum of carbon dioxide has been reported in the  $7123\text{-}7793\text{ cm}^{-1}$  region. In this second contribution, the spectral region investigated by CW-Cavity Ring Down Spectroscopy has been extended up to  $7917\text{ cm}^{-1}$ . It added about 400 lines to our previous list of about 2500 transitions. These additional lines include transitions belonging to six newly observed  $^{12}\text{C}^{16}\text{O}_2$  bands for which we provide the spectroscopic parameters. Over the whole  $7123\text{-}7917\text{ cm}^{-1}$  region, the accurate intensities of about 2900 lines belonging to four isotopologues ( $^{12}\text{C}^{16}\text{O}_2$ ,  $^{13}\text{C}^{16}\text{O}_2$ ,  $^{16}\text{O}^{12}\text{C}^{18}\text{O}$  and  $^{16}\text{O}^{12}\text{C}^{17}\text{O}$ ) were retrieved with an average accuracy of 3 %. Intensity values range between  $1.2\times 10^{-29}$  and  $4.1\times 10^{-25}$  cm/molecule. Compared to the present version of the Carbon Dioxide Spectroscopic Databank recently adopted for the HITRAN database, important deviations were evidenced for some weak bands of the main isotopologue. The CW-CRDS intensity data relative to a total of 46  $^{12}\text{C}^{16}\text{O}_2$  bands together with selected intensity information available in the literature for nine bands have been fitted simultaneously using the effective operators approach. The  $\Delta P=11$  set of the  $^{12}\text{C}^{16}\text{O}_2$  effective dipole moment parameters has been refined leading to a much better agreement with the measured intensity values. In addition, the  $\Delta P=10$  effective dipole moment parameters of the  $^{16}\text{O}^{12}\text{C}^{18}\text{O}$  minor isotopologue were determined for the first time. The obtained results will help to improve the Carbon Dioxide Spectroscopic Databank (CDSDB).

**Key words:** Molecular spectroscopy, Carbon dioxide, Line intensities, Infrared, Global modeling, CW-CRDS, Cavity Ring Down Spectroscopy, Fourier Transform Absorption Spectroscopy, HITRAN, Carbon Dioxide Spectroscopic Databank.

## 1. Introduction

In a first contribution [1], we have reported the line positions analysis of the absorption spectrum of carbon dioxide recorded by CW-Cavity Ring Down Spectroscopy in the 7123-7793  $\text{cm}^{-1}$  spectral interval. A series of 25 fibered distributed feedback (DFB) laser diodes were needed to cover the region and a typical noise equivalent absorption,  $\alpha_{min}$ , of  $3 \times 10^{-10} \text{ cm}^{-1}$  was achieved. 2125 transitions were assigned to the  $^{12}\text{C}^{16}\text{O}_2$ ,  $^{16}\text{O}^{12}\text{C}^{17}\text{O}$  and  $^{16}\text{O}^{12}\text{C}^{18}\text{O}$  isotopologues. These CW-CRDS observations represented a significant improvement in terms of accuracy and sensitivity compared to Venus spectra (about 350 lines) which were the main experimental source for line positions in the region [2]. However, absolute lines intensities cannot be extracted from Venus spectra. A few previous laboratory investigations by Fourier Transform Spectroscopy (FTS) have been dedicated to the line intensity measurements of the strongest  $4\nu_1+\nu_3$  pentad bands dominating the spectrum. In the spectral interval considered here, all the line intensities are smaller than  $5 \times 10^{-25} \text{ cm/molecule}$ . Consequently, kilometeric absorption path lengths were needed by Valero and Boese [3-5] and Giver *et al* [6] to determine line intensities of the  $4001i-00001$  ( $i=1-4$ ) bands. The intensity values of the  $40013-00001$  and  $40014-00001$  bands were also reported by Teffo *et al* from FTS spectra recorded with pressures up to 75.6 Torr and a 40.2 m absorption pathlength [7]. In their paper, Teffo *et al* also reported the line intensity values for the stronger  $10013-00001$  and  $10032-00001$  bands falling above the **presently studied region** (at 8294 and 8192  $\text{cm}^{-1}$  respectively) but belonging to the same  $\Delta P = 11$  series of transitions ( $P = 2\nu_1 + \nu_2 + 3\nu_3$  is the polyad number resulting from approximate relations between the harmonic frequencies). The same situation applies to the line intensities measurement of the  $21122-00001$  perpendicular band and of the  $32211-00001$  “forbidden” band reported by Wattson *et al* during the HITRAN meeting in 1998 [8]. All these FTS data (about 350 intensity values) relative to nine bands in total were the-only experimental source used to fit the effective dipole moment parameters of the  $\Delta P = 11$  series of transitions. In our recent contribution [1], 1653  $^{12}\text{C}^{16}\text{O}_2$  lines were **measured** by CRDS in the 7123-7793  $\text{cm}^{-1}$ . They belong to 37 bands of the  $\Delta P = 11$  series and include 26 hot bands. The reader is referred to Ref. [1] for the rovibrational assignments of the CRDS spectra. The band-by-band analysis of the CRDS spectrum has led to the determination of the rovibrational parameters of a total of 47 bands of the  $^{12}\text{C}^{16}\text{O}_2$ ,  $^{16}\text{O}^{12}\text{C}^{17}\text{O}$  and  $^{16}\text{O}^{12}\text{C}^{18}\text{O}$  isotopologues.

The present report is devoted to the intensity retrieval from the CRDS spectra. By gathering the large set of CRDS intensity values with the previous FTS data, the effective

dipole moment parameters will be refined in the frame of the effective operators approach allowing an improved reproduction of the spectrum in the region.

During the course of this analysis, four additional DFB lasers have been purchased allowing extending the investigation up to  $7917\text{ cm}^{-1}$ . About 400 lines were added to our previous line list. Before the line intensity analysis (Sections 4 and 5), we will present in Section 3 the line positions analysis and the band-by-band fit of the transitions detected in the newly investigated  $7793\text{-}7917\text{ cm}^{-1}$  interval.

## 2. Experimental details

The CW-CRDS spectrometer and the procedure adopted for an accurate calibration of the wavenumber scale have been described in Refs. [9-11]. The DFB typical tuning range is about  $40\text{ cm}^{-1}$  by temperature variation from  $-5^{\circ}\text{C}$  to  $60^{\circ}\text{C}$ . As illustrated in our previous studies in the  $5800\text{-}7000\text{ cm}^{-1}$  region [12, 13], the high linearity and the large dynamic range of the CW-CRDS spectra with respect to the line intensities, makes this technique particularly suitable for intensity measurements. The absolute value of the absorption coefficient,  $\alpha$ , is obtained straightforwardly from the measured ring down time ( $1/\tau - 1/\tau_0 = \alpha c$ ). The pressure, measured by a capacitance gauge (Baratron), as well as the ringdown cell temperature, was monitored during the spectrum recording. The pressure value was generally fixed to  $13.3\text{ hPa}$  ( $10.0\text{ Torr}$ ). In addition, a few recordings were performed at  $5.0\text{ Torr}$  in order to avoid saturation effects of the strongest lines of the  $40013\text{-}00001$  band near  $7600\text{ cm}^{-1}$ . The carbon dioxide sample (purity higher than  $99.998\%$ ) was purchased from Fluka Company and was assumed to be in natural isotopic abundance [13].

In Ref. [1], the  $7123\text{-}7793\text{ cm}^{-1}$  region was covered without any gap with the help of 25 fibered DFB laser diodes. In the present work, the recordings were extended up to  $7917\text{ cm}^{-1}$  with the help of four newly purchased DFB lasers. A different set of high reflective supermirrors was used. Their very high reflectivity (corresponding to  $\tau_0 \approx 150\text{ }\mu\text{s}$  at  $7800\text{ cm}^{-1}$ ) allowed new observations in the  $7650\text{-}7793\text{ cm}^{-1}$  region. On the overview spectrum displayed in Fig. 1, the transitions corresponding to the new recordings are highlighted.

## 3. Line positions analysis in the $7650\text{-}7917\text{ cm}^{-1}$ spectral interval

This region deserves to be accurately characterized as it includes a micro window of high transparency around  $7820\text{ cm}^{-1}$  between the  $40012\text{-}00001$  and  $40011\text{-}00001$  bands (see Fig. 1). The rovibrational assignment and band-by-band analysis followed the procedure described in Ref. [1]. Compared to Ref. [1], nine additional  $^{12}\text{C}^{16}\text{O}_2$  bands could be identified.

They include the 40011-00001 and 21122-00001 bands observed in Venus spectra, for which the rotational analysis was extended and improved. The band-by-band fit of the spectroscopic parameters led to the values listed in Table 1. This table includes all the bands centred above  $7650\text{ cm}^{-1}$  as the parameter values were either newly determined or significantly improved compared to Ref. [1] as a result of new observations. Some of the observed bands are affected by perturbations which were identified on the basis of the effective Hamiltonian models (see last column of Table 1). The deviations from the position values provided in the Carbon Dioxide Spectroscopic Databank (CDS) [16] are plotted versus the line positions in Fig. 1. Important deviations reaching values on the order of  $15 \times 10^{-3}\text{ cm}^{-1}$  are noted for the 42212-02201 and 31123-02201 bands newly observed near  $7775\text{ cm}^{-1}$ .

The new observations were gathered to those of Ref. [1] in order to provide a global and consistent line list. It added 339  $^{12}\text{C}^{16}\text{O}_2$  lines and 14  $^{16}\text{O}^{12}\text{C}^{18}\text{O}$  lines to the set of 1653, 96 and 376 transitions reported in Ref. [1] for the  $^{12}\text{C}^{16}\text{O}_2$ ,  $^{16}\text{O}^{12}\text{C}^{17}\text{O}$  and  $^{16}\text{O}^{12}\text{C}^{18}\text{O}$  isotopologues, respectively. In the global list (2881 lines), provided as Supplementary Material, the experimental positions and intensities as obtained from the line profile fitting (see next section) are given for each line, together with the rovibrational assignments. In order to provide a complete linelist corresponding to natural carbon dioxide, we kept the  $^{13}\text{C}^{16}\text{O}_2$  transitions which are not discussed here.

Compared to the line positions attached to Ref. [1], a better accuracy of the line centers determination has been obtained by using the multiple line fitting program (see next section). That led to marginal changes compared to the line centre values determined in Ref. [1] and to the addition of 102 lines in the spectral region investigated in Ref. [1]. For consistency, we have used these accurate line centers values to refine the spectroscopic parameters of *all* bands of the  $^{12}\text{C}^{16}\text{O}_2$ ,  $^{16}\text{O}^{12}\text{C}^{17}\text{O}$  and  $^{16}\text{O}^{12}\text{C}^{18}\text{O}$  isotopologues reported in Ref. [1]. The obtained parameters values are very close to those of Tables 2-4 of Ref. [1]. They are listed in three Tables provided as Supplementary Material. The results of the band-by-band fit are given for each band as an archive file including the observed and calculated values of the line positions together with the fitted spectroscopic parameters of the upper state with corresponding errors.

#### 4. Line intensity retrieval

The integrated absorption coefficient,  $I$  (in  $\text{cm}^{-2}$ ), was obtained for each line using an interactive least squares multi-lines fitting program. The Levenberg-Marquardt algorithm was used to minimize the deviation between the observed and calculated spectra. For each

individual complete laser scan, the spectral sections of overlapping or nearby transitions that could be treated independently were limited by the fitting program. The contribution of the apparatus function was neglected as the DFB line width is much smaller than the Doppler broadening [1-5 MHz compared to 0.4 GHz (FWHM)]. The  $^{12}\text{CO}_2$  line profile was assumed to be of Voigt type. The position and integrated absorbance of each line, and a baseline (assumed to be a linear or quadratic function of the wavenumber) were provided by the fitting procedure. The Gaussian line widths ( $0.01393\text{ cm}^{-1}$  (FWHM) at  $7500\text{ cm}^{-1}$  for  $^{12}\text{C}^{16}\text{O}_2$ ) were fixed to the theoretical value of the Doppler broadening calculated according to the measured temperature and mass of the considered  $\text{CO}_2$  isotopologue. The Lorentzian line widths were obtained as the product of the sample pressure and the self-broadening coefficients provided in the HITRAN database [14]. They were assumed to be independent of the isotopologue and to decrease smoothly with the rotational quantum number  $J$  (from about  $0.130\text{ cm}^{-1}$  (HWHM) at  $J = 0$  to  $0.0718\text{ cm}^{-1}$  at  $J = 50$ ). The lines due to water vapor, present as an impurity in the sample, were also fitted. Their Gaussian line widths were fixed to the theoretical values while the Lorentzian component was calculated using the  $\text{H}_2\text{O}$  broadening coefficients due to collisions with  $\text{CO}_2$  [15].

Fig. 2 illustrates the large **dynamic range** achieved on the measurement of the line intensities and the quality of the spectrum reproduction. Absorption coefficients ranging from  $5 \times 10^{-10}$  to  $4 \times 10^{-6}\text{ cm}^{-1}$  can be measured from the displayed spectrum.

The absolute line intensity or integrated absorption coefficient per pressure unit,  $\tilde{S}$  (in  $\text{cm}^{-2}\text{ atm}^{-1}$ ), was deduced from the integrated absorption coefficient,  $I(T)$ , using the equation:

$$\tilde{S}(T) = \frac{I(T)}{P} \quad (1)$$

where  $P$  is the pressure of the considered isotopologue (in atm). Each  $\tilde{S}$  value was then converted to the absorption line intensity  $S(T)$  (in  $\text{cm}/\text{molecule}$ ) according to the following expression:

$$S(T) = \frac{1}{N_L} \frac{T}{273.15} \tilde{S}(T) \quad (2)$$

where  $T$  is the sample temperature and  $N_L = 2.68676 \times 10^{19}\text{ molecule cm}^{-3}\text{ atm}^{-1}$  is the Loschmidt number. The temperature value corresponding to our spectra was 296 K with an estimated uncertainty of  $\pm 2\text{ K}$ .

Taking into account all the transitions due to the different species contributing to the spectra ( $^{12}\text{C}^{16}\text{O}_2$ ,  $^{16}\text{O}^{12}\text{C}^{18}\text{O}$ ,  $^{13}\text{C}^{16}\text{O}_2$ ,  $^{16}\text{O}^{12}\text{C}^{17}\text{O}$ ,  $\text{H}_2\text{O}$ ,  $\text{HDO}$ ), more than 4000 lines were fitted. The final set contains the following numbers of intensity values:  $^{12}\text{C}^{16}\text{O}_2$ : 1992,

$^{16}\text{O}^{12}\text{C}^{18}\text{O}$ : 390,  $^{13}\text{C}^{16}\text{O}_2$ : 403 and  $^{16}\text{O}^{12}\text{C}^{17}\text{O}$ : 96. Intensity values range between  $1.22 \times 10^{-29}$  and  $4.11 \times 10^{-25}$  cm/molecule for the main isotopologue. The quality of the spectrum reproduction is illustrated in Figs. 2 and 3. The weakest line displayed on the insert of Fig. 2 has an intensity of  $6.45 \times 10^{-29}$  cm/molecule. The fitting error is less than 1% for well-isolated lines. Taking into account the uncertainties on the temperature ( $296 \pm 2$  K) and pressure ( $\pm 0.5\%$ ) values, we estimated that the accuracy of the line intensities is 2.5% or better for most of the lines. **Note that this error bar does not consider possible deviation from Voigt line shapes and line mixing effect as discussed in Refs. [26-28].**

Fig. 4 shows an overview comparison of the obtained results with the present version of the CDS line list [16] which was adopted for HITRAN2008 [14] in our region. Four bands are observed by CRDS and are missing in the present version of the CDS database while they have an intensity which largely exceeds the CDS intensity cut off ( $10^{-30}$  cm/molecule): (i) the 40013-00001 and 40014-00001 bands of  $^{16}\text{O}^{12}\text{C}^{17}\text{O}$  and (ii) two  $\Delta P = 10$  bands of the  $^{16}\text{O}^{12}\text{C}^{18}\text{O}$  isotopologue which were not predicted in the CDS because the lack of previous observations prevented the determination of the corresponding  $\Delta P = 10$  effective dipole momentum parameters.

The ratios of the measured and CDS line intensities of  $^{12}\text{C}^{16}\text{O}_2$  are plotted in Fig. 5 versus the experimental intensity values. The overall agreement is very good for the strongest bands (the CRDS/CDS average intensity ratio is 1.034 for the line intensities larger than  $10^{-26}$  cm/molecule) but degrades for smaller intensity values. The reduced set of experimental input data [3-8] used to fit the  $\Delta P = 11$  effective dipole moment parameters explains the deviations observed for a number of weak bands. These deviations largely exceed the experimental uncertainty. For instance, the 51104-00001 band at  $7240 \text{ cm}^{-1}$  has line intensities at the  $5 \times 10^{-29}$  cm/molecule level while the CDS intensities are predicted more than five times smaller. This is a consequence of the lack of the respective effective dipole moment parameter. Another clear deviation is noted for the stronger 21123-00001 band (line intensities at the  $10^{-27}$  cm/molecule level) which is predicted about 35 % stronger than observed. Nevertheless, the impact of these disagreements on the total  $^{12}\text{C}^{16}\text{O}_2$  absorbance in the region is very limited: the sum of the CRDS intensities ( $2.079 \times 10^{-23}$  cm/molecule) exceeds by only 3 % the sum of the corresponding CDS intensities. This value is on the same order as our experimental uncertainty.

In the line list provided as Supplementary Material, the experimental and calculated (see below) intensities at 296 K,  $S(T_0)$ , are given for each line. Our list includes 2881 transitions

with intensities ranging between  $1.2 \times 10^{-29}$  and  $4.1 \times 10^{-25}$  cm/molecule. Note that 1451 transitions are predicted in CDSD [16] with an intensity value larger than  $2 \times 10^{-28}$  cm/molecule while 1357 of them were detected, the difference (6.5 %) being mostly due to unrecoverable lines obscured or blended by strong H<sub>2</sub>O transitions below  $7300 \text{ cm}^{-1}$ .

## 5. Modeling and fitting of the line intensities

### *Theoretical approach*

The line intensity,  $S(T)$ , of a vibration-rotation transition  $b \leftarrow a$  is given by the following equation:

$$S_{b \leftarrow a}(T) = \frac{1}{4\pi\epsilon_0} \frac{8\pi^3}{3hc} \frac{Cg_a \nu_{b \leftarrow a}}{Q(T)} \exp\left(-\frac{hcE_a}{kT}\right) \left[1 - \exp\left(-\frac{hc\nu_{b \leftarrow a}}{kT}\right)\right] W_{b \leftarrow a}, \quad (3)$$

where  $\frac{1}{4\pi\epsilon_0} = 10^{-36} \text{ erg cm}^3 \text{ D}^{-2}$ ,  $C$  is the isotopic abundance,  $g_a$  is the nuclear statistical weight of the lower state,  $\nu_{b \leftarrow a}$  is the wavenumber (in  $\text{cm}^{-1}$ ) of the considered transition,  $E_a$  is the energy of the lower state and  $W_{b \leftarrow a}$  is the transition moment squared (in  $\text{D}^2$ ) which is calculated within the framework of the effective operators approach.

The effective operator approach allows the simultaneous modelling of the line intensities of cold and hot bands belonging to the same series of transitions. For the reader's convenience, we briefly recall this approach which has been presented in several of our papers [17-19]. As a result of the approximate relations between the harmonic frequencies

$$\omega_1 \approx 2\omega_2, \quad \omega_3 \approx 3\omega_2 \quad (4)$$

the effective Hamiltonian [20-23] globally describing the line positions of carbon dioxide is formulated with the assumption that the vibration-rotation energy levels can be separated in polyads. The effective Hamiltonian takes into account all resonance interactions between vibration-rotation states belonging to the same polyad, up to the sixth order of the perturbation theory. The polyads are identified with the label:

$$P = 2V_1 + V_2 + 3V_3, \quad (5)$$

where  $V_i$  are vibrational quantum numbers.

Within the effective operators approach, the square of the transition dipole moment of a vibration-rotation transition  $P'N'J'\epsilon' \leftarrow PNJ\epsilon$  is given by [17-19]:

$$W_{P'N'J'\varepsilon'\leftarrow PNJ\varepsilon} = (2J+1) \left| \sum_{V_1 V_2 \ell_2 V_3} \sum_{\substack{2\Delta V_1 + \Delta V_2 + 3\Delta V_3 = \Delta P \\ \Delta \ell_2 = 0, \pm 1, \pm 2, \dots}} J C_{PN\varepsilon}^{V_1 V_2 \ell_2 V_3} J' C_{P'N'\varepsilon'}^{V_1 + \Delta V_1 V_2 + \Delta V_2 \ell_2 + \Delta \ell_2 V_3 + \Delta V_3} M_{\Delta V}^{|\Delta \ell_2|} \right. \\ \left. \times \sqrt{f_{\Delta V}^{\Delta \ell_2}(V, \ell_2) (1 + \delta_{\ell_2, 0} + \delta_{\ell_2, 0} - 2\delta_{\ell_2, 0} \delta_{\ell_2, 0})} \Phi_{\Delta, \Delta \ell_2}(J, \ell_2) \left( 1 + \sum_i \kappa_i^{\Delta V} V_i + F_{\Delta V}^{\Delta \ell_2}(J, \ell_2) \right) \right|^2 \quad (6)$$

Here  $\delta_{i,j}$  is the Kronecker symbol and  $J C_{PN\varepsilon}^{V_1 V_2 \ell_2 V_3}$  stands for the expansion coefficient determining the eigenfunction of the lower state:

$$\Psi_{PNJ\varepsilon}^{eff} = \sum_{\substack{2V_1 + V_2 + 3V_3 = P \\ \ell_2}} J C_{PN\varepsilon}^{V_1 V_2 \ell_2 V_3} |V_1 V_2 | \ell_2 | V_3 J \varepsilon \rangle \quad (7)$$

The summation runs over all states within the polyad involved. The definition of the Wang-type basis functions  $|V_1 V_2 | \ell_2 | V_3 J \varepsilon \rangle$  is given, for example, in Ref. [17]. In the same way,  $J' C_{P'N'\varepsilon'}^{V_1 V_2 \ell_2 V_3}$  stands for the expansion a coefficient within the upper-state polyad. The functions  $\Phi_{\Delta, \Delta \ell_2}(J, \ell_2)$  for  $\Delta \ell_2 = 0, \pm 1$  are equal to the Clebsh-Gordon coefficients  $(1 \Delta \ell_2 J \ell_2 | (J + \Delta J)(\ell_2 + \Delta \ell_2))$ , related to the Hönl-London factors by the equation

$$\left( (1 \Delta \ell_2 J \ell_2 | (J + \Delta J)(\ell_2 + \Delta \ell_2)) \right)^2 = \frac{L_{\Delta V}^{\Delta \ell_2}}{2J+1} \quad (8)$$

The  $f_{\Delta V}^{\Delta \ell_2}(V, \ell_2)$  functions are listed in Table 1 of Ref. [17] for small values of the quantum number differences  $\Delta V$ . The Herman-Wallis-type functions  $F_{\Delta V}^{\Delta \ell_2}(J, \ell_2)$  appearing in Eq. (6) are given in Ref. [18]. The following terms were needed in the present paper:

$$F_{\Delta V}^{\Delta \ell_2}(J, \ell_2) = b_J^{\Delta V} m \quad (9)$$

for the  $\Delta \ell_2 = 0$  matrix elements,

$$F_{\Delta V}^{\Delta \ell_2}(J, \ell_2) = -\frac{1}{2} b_J^{\Delta V} (2\ell_2 \Delta \ell_2 + 1) \quad (10)$$

for the  $\Delta J = 0$ ,  $\Delta \ell_2 = \pm 1$  matrix elements, and

$$F_{\Delta V}^{\Delta \ell_2}(J, \ell_2) = -\frac{1}{2} b_J^{\Delta V} (2\ell_2 \Delta \ell_2 + 1) + b_J^{\Delta V} m \quad (11)$$

for  $\Delta J = \pm 1$ ,  $\Delta \ell_2 = \pm 1$  matrix elements.

The  $M_{\Delta V}^{|\Delta \ell_2|}$ ,  $\kappa_i^{\Delta V}$  ( $i= 1-3$ ), and  $b_J^{\Delta V}$  parameters of the effective dipole moment matrix elements involved in Eqs. (6) and (9)-(11) describe simultaneously the intensities of all the

lines of cold and hot bands belonging to a series of transitions characterized by a given  $\Delta P$  value. These parameters were fitted to the observed line intensities.

### *Line intensities fitting*

Using the above approach, we have performed the least-squares fittings of the line intensities for the  $\Delta P=10$  series of transitions of the  $^{16}\text{O}^{12}\text{C}^{18}\text{O}$  isotopologue and for the  $\Delta P=11$  series of transitions of the principal isotopologue,  $^{12}\text{C}^{16}\text{O}_2$ . In the CRDS line list attached as Supplementary Material, the lines included in the respective fits are indicated.

The aim of the fitting procedure is to minimize the dimensionless weighted standard deviation  $\chi$ , defined according to the usual formula

$$\chi = \sqrt{\frac{\sum_{i=1}^N \left( \frac{S_i^{obs} - S_i^{calc}}{\delta_i} \right)^2}{(N - n)}}, \quad (12)$$

where  $S_i^{obs}$  and  $S_i^{calc}$  are, respectively, observed and calculated values of the intensity for the  $i$ -th line;  $\delta_i = \frac{S_i^{obs} \sigma_i}{100\%}$ , where  $\sigma_i$  is the measurement error of the  $i$ -th line in %,  $N$  is the number of fitted line intensities, and  $n$  is the number of adjusted parameters. To characterize the quality of a fit, we also use the root mean square (RMS) deviation, defined according to the equation

$$RMS = \sqrt{\frac{\sum_{i=1}^N \left( \frac{S_i^{obs} - S_i^{calc}}{S_i^{obs}} \right)^2}{N}} \times 100\%. \quad (13)$$

### *$\Delta P=10$ series of transitions of $^{16}\text{O}^{12}\text{C}^{18}\text{O}$*

The very weak 20021-00001 and 20022-00001 bands of  $^{16}\text{O}^{12}\text{C}^{18}\text{O}$  are absent in the line lists of provided by CDS [16] and HITRAN2008 [14] as the intensities of these  $\Delta P=10$  bands were unknown before the present measurements. Their measured line intensities allowed us to fit two effective dipole moment parameters of this series of transitions.

Very weak lines and those overlapped and blended were excluded from the fit leaving 65 from a total of 97 intensity values. The following weighting of the input data was adopted: the uncertainties of the intensities of the lines weaker than  $10^{-28}$  cm/molecule were assumed to be 6% while a value of 3% was adopted for the others, in accordance with the estimates performed in the experimental part of this paper. The values of the expansion coefficients

$J C_{PN\epsilon}^{V_1 V_2 \ell_2 V_3}$  of the eigenfunctions have been obtained from the global fit of the effective

Hamiltonian parameters to the observed line positions. The same set of effective Hamiltonian parameters was used as the one used to generate the CDSDB databank [16]. The partition functions  $Q(T)$  and nuclear statistical weights were taken from Ref. [24]. The result of the fit is presented in Table 2 and in Table 3. The fitted set of effective dipole moment parameters is given in Table 4. The weighted standard deviation  $\chi = 1.4$  and global RMS=5.3% show that the fit is performed near experimental accuracy.

*$\Delta P=11$  series of transitions of  $^{12}\text{C}^{16}\text{O}_2$*

The set of the effective dipole moment parameters used for the generation of the line intensities of this series of transitions for the CDSDB databank has been published in Ref.[7]. The parameters were fitted to the line intensities measured from FTS spectra in Refs. [3, 4, 6-8]. The characteristics of these data are summarized in Table 3. Note that this FTS dataset includes transitions of the strong  $\nu_1+3\nu_3$  dyad ( $\Delta P=11$ ) located between  $8150\text{ cm}^{-1}$  and  $8310\text{ cm}^{-1}$  [7] *ie* above the region presently investigated by CRDS. As illustrated in Fig. 5, the obtained set of the effective dipole moment parameters do not reproduce satisfactorily the line intensities of some newly measured weak bands and should be refined. The CW-CRDS intensity data relative to  $^{12}\text{C}^{16}\text{O}_2$  (1650 values) together with the FTS intensity values (about 260 values in total) have been used to refine the  $\Delta P=11$  effective dipole parameters of the principal isotopologue.

In our new fit, the line intensities were weighted according to their assumed uncertainties,  $\sigma_i$ , which are based on the **declared uncertainties**. When in a respective experimental source, each individual line was supplied with its uncertainty; this uncertainty was used in the fit. Otherwise, we used the averaged uncertainty values as given in Table 2. The line intensities of the 41112- 01101 hot band published in Ref. [4] were excluded from the fit because of their very large reported uncertainties. Again very weak, overlapped and blended lines were excluded from the set of 1992 CRDS intensity values of  $^{12}\text{C}^{16}\text{O}_2$  leaving 1651 values included in the fit. The same weighting as in the case of the  $\Delta P=10$  series of transitions of  $^{16}\text{O}^{12}\text{C}^{18}\text{O}$  was adopted: uncertainties of 3 and 6 % were affected to the intensity values above and below  $10^{-28}\text{ cm/molecule}$ , respectively. The values of the expansion coefficients  $J C_{PN\epsilon}^{V_1 V_2 \ell_2 V_3}$  of the eigenfunctions have been obtained using the effective Hamiltonian which was used for the generation of CDSDB databank [16]. The partition functions  $Q(T)$  and nuclear statistical weights were taken from Ref. [24]. The result of the fit is presented in Table 2 and in Table 3. The fitted set of effective dipole moment parameters is given in Table 4. The quality of this fit is very similar to that described above for the  $\Delta P=10$

series in  $^{16}\text{O}^{12}\text{C}^{18}\text{O}$ : weighted standard deviation  $\chi = 1.3$  and global RMS= 4.9%. Fig. 5 illustrates the improvement compared to the present CDS line list.

The new set of the effective dipole moment parameters for  $\Delta P=11$  series of transitions in  $^{12}\text{C}^{16}\text{O}_2$  has additional parameters compared to the previous one [7]. These additional parameters are very important for the calculation of the line intensities of some weak perpendicular bands. As concerns of other principal parameters  $M$  of the matrix elements of the effective dipole moment operator, they are not very different but the parameters describing vibrational ( $\kappa$ ) and rotational ( $b_J$ ) dependences of the principal parameters differ considerably in the old and new sets of parameters. The reason is evident. Due to the sensitivity achieved by CW-CRDS, the measurements of the line intensities has been extended to a large number of hot bands and to much higher values of the rotational quantum number  $J$ . These changes of the parameters values may have an important impact on the calculations of the  $^{12}\text{C}^{16}\text{O}_2$  at hot temperature.

#### *Global linelist*

The global list of 2881 lines attached as Supplementary Material is relative to carbon dioxide in natural abundance and provides line parameters for the four isotopologues contributing to the CRDS spectrum in the 7123-7917  $\text{cm}^{-1}$  region. Together with the rovibrational assignment, experimental positions and intensities, it includes the calculated intensities values except for the  $^{13}\text{C}^{16}\text{O}_2$  isotopologue which will be treated in a separate contribution. For the  $\Delta P=11$  series of the principal isotopologue and for the  $\Delta P=10$  series of  $^{16}\text{O}^{12}\text{C}^{18}\text{O}$ , the line intensities are those calculated with the presently fitted set of effective dipole parameters. In the case of the  $\Delta P=11$  series of both  $^{16}\text{O}^{12}\text{C}^{18}\text{O}$  and  $^{16}\text{O}^{12}\text{C}^{17}\text{O}$ , the intensity values were calculated using the corresponding set of the principal isotopologue. Fig. 6 shows that, compared to the present intensity values provided in CDS (and in HITRAN2008), the new set of  $^{12}\text{C}^{16}\text{O}_2$  parameters allows improving significantly the intensity reproduction of the  $\Delta P=11$  series of  $^{16}\text{O}^{12}\text{C}^{18}\text{O}$ . The agreement could be slightly improved by a fit of the  $\Delta P=11$  effective dipole parameters of  $^{16}\text{O}^{12}\text{C}^{18}\text{O}$ . This work will be included in a separate contribution devoted to the  $^{16}\text{O}^{12}\text{C}^{18}\text{O}$  and  $^{16}\text{O}^{12}\text{C}^{17}\text{O}$  intensity measurements and modelling in the whole 5850-7917  $\text{cm}^{-1}$  region.

## **6. Conclusion**

Extensive line intensity measurements of the carbon dioxide molecule have been performed in the 7123-7917  $\text{cm}^{-1}$  region using the CW-CRDS spectrometer developed in

Grenoble. This spectrometer allowed measurements of the line intensities of both very weak and strong lines (from  $1.22 \times 10^{-29}$  up to  $4.11 \times 10^{-25}$  cm/molecule). 2881 lines of four isotopologues -  $^{12}\text{C}^{16}\text{O}_2$ ,  $^{16}\text{O}^{12}\text{C}^{18}\text{O}$ ,  $^{13}\text{C}^{16}\text{O}_2$  and  $^{16}\text{O}^{12}\text{C}^{17}\text{O}$  - have been retrieved with an average uncertainty of 3%. The majority of these line intensities were measured for the first time. Compared to our previous paper [1] the accessible wavenumber region was extended from 7793 to 7917  $\text{cm}^{-1}$ . It gave us the possibility to detect about 400 additional lines of carbon dioxide in the 1.35  $\mu\text{m}$  region and to observe six new  $^{12}\text{C}^{16}\text{O}_2$  bands for which the spectroscopic parameters are provided.

Using the newly measured line intensities, the effective dipole moment parameters of the  $\Delta P=10$  series of transitions in  $^{16}\text{O}^{12}\text{C}^{18}\text{O}$  were fitted. The previous set [7] of effective dipole moment parameters of the  $\Delta P=11$  series of transitions in the principal isotopologue was refined leading to important differences for the parameters values describing the vibrational and rotational dependences. These refined sets of effective dipole moment parameters allow reproducing all measured line intensities including those of very weak bands with accuracy close to the experimental uncertainties.

The obtained results will be used to improve the CDSD databank [16].

### **Acknowledgments**

This work is jointly supported by CNRS (France), RFBR (Russia, grant N 09-05-93105) and CAS (China) in the frame of Groupement de Recherche International SAMIA (Spectroscopy of Molecules of Atmospheric Interest).

## References

- [1] Kassi S, Song K, Campargue A High Sensitivity CW-Cavity Ring Down Spectroscopy of  $^{12}\text{CO}_2$  near 1.35  $\mu\text{m}$  (I): Line positions. JQSRT doi:10.1016/j.jqsrt.2009.04.010.
- [2] Mandin JY. Interpretation of the  $\text{CO}_2$  absorption bands observed in the Venus infrared spectrum between 1 and 2.5  $\mu\text{m}$ . J Mol Spectrosc 1977;67:304-21.
- [3] Valero FPJ. Absolute intensity measurements of the  $\text{CO}_2$  bands  $401_{\text{III}}\leftarrow 000$  and  $411_{\text{III}}\leftarrow 010$ . J Mol Spectrosc 1977;68:269-79.
- [4] Valero FPJ, Boese RW. The absorption spectrum of  $\text{CO}_2$  around 7740  $\text{cm}^{-1}$ . JQSRT 1977;18:391-8.
- [5] Valero FPJ, Boese RW. Comments on the note by Arié et al. On the transition moment of the  $\text{CO}_2$  band near 7740  $\text{cm}^{-1}$ . JQSRT 1978;20:427.
- [6] Giver LP, Chackerian C, Spencer MN, Brown LR, Wattson RB. The Rovibrational Intensities of the  $(40^0_1) \leftarrow (00^0_0)$  Pentad Absorption Bands of  $^{12}\text{C}^{16}\text{O}_2$  between 7284 and 7921  $\text{cm}^{-1}$ . J Mol Spectrosc 1996;175:104-11.
- [7] Teffo JL, Claveau C, Kou Q, Guelachvili G, Ubelmann A, Perevalov VI, Tashkun SA. Line Intensities of  $^{12}\text{C}^{16}\text{O}_2$  in the 1.2–1.4  $\mu\text{m}$  Spectral Region. J Mol Spectrosc 2000;201:249-55.
- [8] Wattson RB, Giver LP, Kshirsagar RJ, Freedman RS, Chackerian Jr C. Direct numerical diagonalization line-by-line calculations compared to line parameters in several weak interacting  $\text{CO}_2$  bands near 7901  $\text{cm}^{-1}$ . Fifth Bienial HITRAN Conference. Bedford, MA, USA, 1998. P. 29.
- [9] Ding Y, Macko P, Romanini D, Perevalov VI, Tashkun SA, Teffo JL, Hu SM, Campargue A. High sensitivity cw-cavity ringdown and Fourier transform absorption spectroscopies of  $^{13}\text{CO}_2$ . J Mol Spectrosc 2004;226:146-160.
- [10] Morville J, Romanini D, Kachanov AA, Chenevier M. Two schemes for trace detection using cavity ringdown spectroscopy. Appl Phys 2004;D78:465-76.
- [11] Macko P, Romanini D, Mikhailenko SN, Naumenko OV, Kassi S, Jenouvrier A, Tyuterev VG. High sensitivity CW-cavity ring down spectroscopy of water in the region of the 1.5  $\mu\text{m}$  atmospheric window. J Mol Spectrosc 2004;227:90-108.
- [12] Perevalov BV, Deleporte T, Liu AW, Kassi S, Campargue A, Vander Auwera J, Tashkun SA, and Perevalov VI. Global modeling of  $^{13}\text{C}^{16}\text{O}_2$  absolute line intensities from CW-CRDS and FTS measurements in the 1.6 and 2.0 micrometer regions. JQSRT 2008;109:2009-26.
- [13] Perevalov BV, Campargue A, Gao B, Kassi S, Tashkun SA, Perevalov VI. New CW-CRDS measurements and global modeling of  $^{12}\text{C}^{16}\text{O}_2$  absolute line intensities in the 1.6  $\mu\text{m}$  region. J Mol Spectrosc 2008;252:190-7.

- [14] Rothman LS, Gordon IE, Barbe A, Benner DC, Bernath PF et al. The HITRAN 2008 Molecular Spectroscopic Database. *JQSRT* 2009;110:533-72.
- [15] Lavrentieva NN, private communication.
- [16] Perevalov VI, Tashkun SA. CDS-296 (Carbon Dioxide Spectroscopic Databank): Updated and Enlarged Version for Atmospheric Applications. 10th HITRAN Database Conference, Cambridge MA, USA, 2008. <http://cdsd.iao.ru>
- [17] Perevalov VI, Lobodenko EI, Lyulin OM, Teffo JL. Effective dipole moment and band intensities problem for carbon dioxide. *J Mol Spectrosc* 1995;171:435-52.
- [18] Teffo JL, Lyulin OM, Perevalov VI, Lobodenko EI. Application of the effective operator approach to the calculation of  $^{12}\text{C}^{16}\text{O}_2$  line intensities. *J Mol Spectrosc* 1998;187:28-41.
- [19] Tashkun SA, Perevalov VI, Teffo JL, Tyuterev VG. Global fit of  $^{12}\text{C}^{16}\text{O}_2$  vibrational-rotational line intensities using the effective operator approach. *JQSRT* 1999;62:571-98.
- [20] Chédin A. The carbon dioxide molecule. Potential, spectroscopic, and molecular constants from its infrared spectrum. *J Mol Spectrosc* 1979;76: 430-91.
- [21] Teffo JL, Sulakshina ON, Perevalov VI. Effective Hamiltonian for rovibrational energies and line intensities of carbon dioxide. *J. Mol. Spectrosc.* 156 (1992) 48-64.
- [22] Tashkun SA, Perevalov VI, Teffo JL, Rothman LS, Tyuterev VG. Global fitting of  $^{12}\text{C}^{16}\text{O}_2$  vibrational-rotational line positions using the effective Hamiltonian approach. *JQSRT* 1998;60:785-801.
- [23] Tashkun SA, Perevalov VI, Teffo JL, Lecoutre M, Huet TR, Campargue A, Bailly D, Esplin MP.  $^{13}\text{C}^{16}\text{O}_2$ : Global treatment of vibrational-rotational spectra and first observation of the  $2\nu_1 + 5\nu_3$  and  $\nu_1 + 2\nu_2 + 5\nu_3$  absorption bands. *J Mol Spectrosc* 2000;200:162-76.
- [24] Fischer J, Gamache RR, Goldman A, Rothman LS, Perrin A. Total internal partition sums for molecular species in the 2000 edition of the HITRAN database. *JQSRT* 2003;82:401-12.
- [25] Miller CE, Brown LR. Near infrared spectroscopy of carbon dioxide I.  $^{16}\text{O}^{12}\text{C}^{16}\text{O}$  line positions. *J Mol Spectrosc* 2004;228:329-54.
- [26] Malathy Devi V, Chris Benner D, Brown LR, Miller CE, Toth RA. Line mixing and speed dependence in  $\text{CO}_2$  at  $6227.9\text{ cm}^{-1}$ : Constrained multispectrum analysis of intensities and line shapes in the  $30013 \leftarrow 00001$  band. *J Mol Spectrosc* 2007;245:52-80.
- [27] Casa G, Wher R, Castrillo A, Fasci, Gianfrani L. The line shape problem in the near-infrared spectrum of self colliding  $\text{CO}_2$  molecules: experimental investigation and test of semiclassical models. *J Chem Phys* 2009;130:184306.

[28] Predoi-Cross A, Unni AV, Liu W, Schofield I, Holladay C, McKellar ARW, Hurtmans D. Line shape parameters measurement and computations for self-broadened carbon dioxide transitions in the 30012 ← 00001 and 30013 ← 00001 bands, line mixing, and speed dependence *J Mol Spectrosc* 2007;245:34–51.

## Figure captions

**Figure 1.** *Upper panel:* Overview of the  $^{12}\text{C}^{16}\text{O}_2$  spectrum recorded by CW-CRDS between 7123 and 7917  $\text{cm}^{-1}$ . Full and open circles correspond to transitions reported in Ref. [1] and in the present work, respectively.

*Lower panel:* Differences between the measured line positions and those provided by the CDSDB databank (adopted for HITRAN 2008).

**Figure 2.** The CW-CRDS spectrum of carbon dioxide ( $P= 6.65$  hPa) in the region of head of the  $R$  branch of the 40013–00001 band centred at 7594  $\text{cm}^{-1}$ . Three successive enlargements show that line intensities differing by three orders of magnitude can be retrieved from the displayed spectrum. The left and right hand panels illustrate the agreement between the CW-CRDS spectrum and its simulation.

**Figure 3.** Comparison of the CW-CRDS spectrum of carbon dioxide ( $P= 6.65$  hPa) near 7593  $\text{cm}^{-1}$  with its simulation:

*Upper panel:* Experimental spectrum,

*Medium panel:* Simulated spectrum resulting from the fitting procedure,

*Lower panel:* Residuals between the simulated and experimental spectra.

Note the change of the ordinate scale.

**Figure 4.** Overview spectrum of the different isotopologues of carbon dioxide in the 7080 – 7920  $\text{cm}^{-1}$  region. Note the logarithmic scale adopted for the line intensities.

*Left panel:* calculated line list of the Carbon Dioxide Spectroscopic Databank [16],

*Right panel:* experimental line list obtained from the analysis of CW-CRDS spectrum. The two  $\Delta P=10$  bands of  $^{16}\text{O}^{12}\text{C}^{18}\text{O}$  which are highlighted are missing in the present version of the CDSDB linelist (see Text).

**Figure 5.** Variation of the ratio of the experimental and calculated intensities versus the experimental intensity values of the  $^{12}\text{C}^{16}\text{O}_2$  transitions in the 7123-7917  $\text{cm}^{-1}$  region. A different symbol is used for each experimental work (open triangles correspond to the CRDS measurements while the other symbols are relative to the FTS measurements of Refs [3-8]. Only lines included in the fit of the effective dipole parameters are shown (see Text). Note that some CDSDB intensities of the 51104-00001 band at 7240  $\text{cm}^{-1}$  are predicted more than

five times smaller than observed and the corresponding ratios are out of scale of the left hand panel.

*Left panel:* the calculated intensities are those of the present version of the Carbon Dioxide Spectroscopic Databank [16] adopted for HITRAN2008 [14],

*Right panel:* the calculated intensities are those obtained in this work after refinement of the  $\Delta P=11$  effective dipole moment parameters.

**Figure 6.** Variation of the ratio of the experimental and calculated intensities versus the experimental intensity values of the  $^{16}\text{O}^{12}\text{C}^{18}\text{O}$  transitions in the 7123-7917  $\text{cm}^{-1}$  region. A different colour is used for the different bands. Only unblended lines are shown (see Text).

*Left panel:* the calculated intensities are those of the present version of the Carbon Dioxide Spectroscopic Databank [16] adopted for HITRAN2008 [14],

*Right panel:* the calculated intensities are those obtained in this work by using the refined values of the effective dipole moment parameters of the main isotopologue,  $^{12}\text{C}^{16}\text{O}_2$ .

**Table 1.** Spectroscopic parameters (in  $\text{cm}^{-1}$ ) of the  $^{12}\text{C}^{16}\text{O}_2$  bands obtained from the analysis of the CW-CRDS spectrum above  $7650 \text{ cm}^{-1}$  region. The bold characters are used for the bands which were note reported in Ref. [1]. When available, the previous determinations of the parameters values are given in italics.

$P'-P''$	Band	$\Delta G_v$	$G_v$	$B_v$	$D_v \times 10^7$	$H_v \times 10^{12}$	$rms \times 10^3$	$N_{FIT}/N_{TOT}$	$J_{MAX}^{P/Q/R}$	Notes
13-2	50013e-10002e	7679.80697(14)	8965.21508(14)	0.38589984(40)	0.7281(21)		0.45	44/45	43/ / 47	
12-1	22223e-01101e							/3		
12-1	22223f-01101e							/4		
12-1	22223e-01101f							/1		
12-1	22223f-01101f							/2		
11-0	32212e-00001e	7694.40208(92)	7694.40208(92)	0.3882964(12)	1.5312(35)		0.86	25/28	49/ / 55	Forbidden band. Only high $J$ values observed.
<b>14-3</b>	<b>51113e-11102e</b>							/3		
<b>14-3</b>	<b>51113f-11102f</b>							/1		
11-0	40012e-00001e	7734.44903(22)	7734.44903(22)	0.3869481(11)	0.703(12)	-9.55(35)	0.67	47/69	67/ / 71	High $J$ value not fitted 21123e $\leftrightarrow$ 40012 Coriolis resonance interaction. Energy level crossing at $J=68$ .
<i>11-0</i>	<i>40012e-00001e</i>	<i>7734.4478(23)</i>		<i>0.3869970(46)</i>	<i>1.151(17)</i>		8.58		59/ / 67	<i>Mandin [2]</i>
<i>11-0</i>	<i>40012e-00001e</i>	<i>7734.4477160(74)</i>		<i>0.386961162(30)</i>	<i>0.922856(237)</i>		1.37		37	<i>Miller and Brown [25]</i>
11-0	21123e-00001e	7743.69624(25)	7743.69624(25)	0.3853190(11)	1.646(12)	10.62(34)	0.69	43/60	65/ / 67	High $J$ value not fitted 21123e $\leftrightarrow$ 40012 Coriolis resonance interaction. Energy level crossing at $J=68$ .
<i>11-0</i>	<i>21123e-00001e</i>	<i>7743.7131(75)</i>		<i>0.3852016(286)</i>			13.1		9/22/49	<i>Mandin [2]</i>
11-0	21123f-00001e	7743.69672(19)	7743.69672(19)	0.38652351(93)	1.766(10)	0.55(30)	0.35	21/22	/ 50/	
13-2	50012e-10001e	7749.60576(27)	9137.78985(27)	0.3877856(12)	0.651(13)	3.37(39)	0.66	38/40	43/ / 49	
12-1	41112e-01101e	7757.61923(17)	8424.99906(17)	0.38682119(53)	1.0200(37)	0.685(68)	0.57	58/58	56/ / 62	
<i>12-1</i>	<i>41112e-01101e</i>	<i>7757.6253(22)</i>		<i>0.3868226(655)</i>	<i>0.999(4)</i>		0.75		41/ / 45	<i>Mandin [2]</i>
12-1	41112e-01101f							/8		
12-1	41112f-01101e							/7		
12-1	41112f-01101f	7757.61937(17)	8424.99919(17)	0.38851959(57)	0.9512(43)	-0.362(87)	0.54	55/57	55/ / 61	
<i>12-1</i>	<i>41112f-01101f</i>	<i>7757.6250(47)</i>		<i>0.3869970(46)</i>	<i>0.940(11)</i>		1.46		41/ / 45	<i>Mandin [2]</i>
<b>14-3</b>	<b>51112e-11101e</b>							/2		
<b>14-3</b>	<b>51112f-11101f</b>							/2		
13-2	42212e-02201e	7772.9396(11)	9108.0710(11)	0.387802(24)	11.0(11)		0.71	10/36	35/ / 43	perturbed band, 42212 $\leftrightarrow$ 31123 Coriolis resonance

13-2	42212f-02201e							/1		interaction. No energy level crossing.
13-2	42212f-02201f	7772.93662(66)	9108.06801(66)	0.3878568(77)	7.77(17)		0.89	13/23	30/ / 44	perturbed band, 42212↔31123 Coriolis resonance interaction. No energy level crossing.
<b>13-2</b>	<b>31123f-02201f</b>							<b>/12</b>		perturbed band 42212↔31123 Coriolis resonance interaction. No energy level crossing.
<b>13-2</b>	<b>31123e-02201e</b>							<b>/13</b>		perturbed band 42212↔31123 Coriolis resonance interaction. No energy level crossing.
<b>12-1</b>	<b>30023e-01101e</b>	<b>7821.02802(95)</b>	<b>8488.40785(95)</b>	<b>0.3838392(49)</b>	<b>1.786(67)</b>	<b>1.7(26)</b>	<b>0.70</b>	<b>16/16</b>	<b>0/ / 40</b>	
<b>12-1</b>	<b>30023e-01101f</b>	<b>7821.02850(48)</b>	<b>8488.40833(48)</b>	<b>0.3838332(26)</b>	<b>1.724(26)</b>		<b>0.72</b>	<b>12/14</b>	<b>/ 32/</b>	
<b>11-0</b>	<b>51101e-00001e</b>	<b>7847.8206(23)</b>	<b>7847.8206(23)</b>	<b>0.3898772(73)</b>	<b>0.978(68)</b>	<b>7.9(19)</b>	<b>0.70</b>	<b>13/20</b>	<b>37/ / 47</b>	
<b>12-1</b>	<b>22222e-01101e</b>	<b>7877.00773(25)</b>	<b>8544.38756(25)</b>	<b>0.38550087(69)</b>	<b>1.4020(33)</b>		<b>0.45</b>	<b>15/16</b>	<b>/ / 46</b>	
<b>12-1</b>	<b>22222f-01101e</b>	<b>7877.00546(46)</b>	<b>8544.38529(46)</b>	<b>0.3855059(33)</b>	<b>1.466(54)</b>	<b>2.4(23)</b>	<b>0.70</b>	<b>17/18</b>	<b>/39/</b>	
<b>12-1</b>	<b>22222e-01101f</b>	<b>7877.00633(35)</b>	<b>8544.38615(35)</b>	<b>0.3855006(14)</b>	<b>1.388(10)</b>		<b>0.70</b>	<b>16/18</b>	<b>/38/</b>	
<b>12-1</b>	<b>22222f-01101f</b>	<b>7877.00713(28)</b>	<b>8544.38696(28)</b>	<b>0.38550125(87)</b>	<b>1.3955(33)</b>		<b>0.60</b>	<b>15/18</b>	<b>13/ / 51</b>	
<b>11-0</b>	<b>32211e-00001e</b>	<b>7897.5422(27)</b>	<b>7897.5422(27)</b>	<b>0.388987(19)</b>	<b>11.79(30)</b>		<b>0.72</b>	<b>7/15</b>	<b>29/ / 25</b>	perturbed band, 32211e↔21122e Coriolis resonance interaction. Energy level crossing at $J=29$ .
<b>11-0</b>	<b>32211f-00001e</b>							<b>/10</b>		32211f↔21122f Coriolis resonance interaction. Energy level crossing at $J=32$ .
<b>11-0</b>	<b>21122e-00001e</b>	<b>7901.47050(53)</b>	<b>7901.47050(53)</b>	<b>0.3842956(99)</b>	<b>2.42(45)</b>	<b>1330.(54)</b>	<b>0.82</b>	<b>21/28</b>	<b>37/ / 23</b>	perturbed band, 32211e↔21122e Coriolis resonance interaction. Energy level crossing at $J=29$ .
<i>11-0</i>	<i>21122e-00001e</i>	<i>7901.613(71)</i>		<i>0.383800 (117)</i>	<i>1.57(100)</i>				<i>24/48/50</i>	<i>Mandin [2]</i>
<b>11-0</b>	<b>21122f-00001e</b>							<b>/17</b>		perturbed band, 32211f↔21122f Coriolis resonance interaction. Energy level crossing at $J=32$ .
<b>11-0</b>	<b>40011e-00001e</b>	<b>7920.83157(32)</b>	<b>7920.83157(32)</b>	<b>0.3885497(10)</b>	<b>0.5360(73)</b>	<b>1.60(14)</b>	<b>0.59</b>	<b>25/26</b>	<b>59/ /</b>	
<i>11-0</i>	<i>40011e-00001e</i>	<i>7920.8383(2)</i>		<i>0.3885500(13)</i>	<i>0.550(17)</i>		<i>0.66</i>		<i>44/ /48</i>	<i>Mandin [2]</i>

### Notes.

$RMS$ : Standard deviation of the fit of the rovibrational parameters

$N_{FIT}$ : number of line positions included in the fit.

$N_{CRDS}$ : number of line positions observed by CW-CRDS in the present work

$N_{TOTAL}$ : total number of line positions assigned to the considered bands.

$J_{MAX}$ : maximum value of the rotational quantum number of the assigned transitions.

The spectroscopic parameters of the lower states were taken from Ref. [25].

**Table 2.** Experimental data and results of the global fits.

Reference	Region (cm <sup>-1</sup> )	Accuracy (%)	$N^{(a)}$	RMS(%) <sup>(b)</sup>
	$^{16}\text{O}^{12}\text{C}^{18}\text{O}$ $\Delta P=10$ series			
This work	7123-7322	3-6	65	5.3
	$^{12}\text{C}^{16}\text{O}_2$ $\Delta P=11$ series			
Valero [3]	7548-7617	2-11	49	5.7
Valero and Boese [4,5]	7698-7760	1-5	21	4.1
Giver et al [6]	7422-7951	2-10	60	3.1
Wattson et al [7]	7885-7925	10	38	6.3
Teffo et al [8]	7474-8310	3	93	2.2
This work	7123-7917	3-6	1650	5.0

<sup>(a)</sup>  $N$  - number of fitted line intensities, <sup>(b)</sup> RMS - corresponding residuals.

**Table 3.** Summary of the line intensity fits.

Series	Number of lines	Number of bands	$J_{\max}$	$S_{\min}^a$	$S_{\max}^a$	$\chi$	RMS (%)	$n^b$
$^{16}\text{O}^{12}\text{C}^{18}\text{O}$ $\Delta P=10$	65	2	42	$1.84 \times 10^{-29}$	$2.66 \times 10^{-28}$	1.4	5.3	2
$^{12}\text{C}^{16}\text{O}_2$ $\Delta P=11$	1911	45	76	$1.53 \times 10^{-29}$	$2.43 \times 10^{-24}$	1.3	4.9	15

<sup>(a)</sup>  $S_{\min}$  and  $S_{\max}$  (in cm/molecule) are the minimum and maximum values of line intensity included into the fit.

<sup>(b)</sup>  $n$  is the number of adjusted parameters.

**Table 4.** Effective dipole moment parameters.

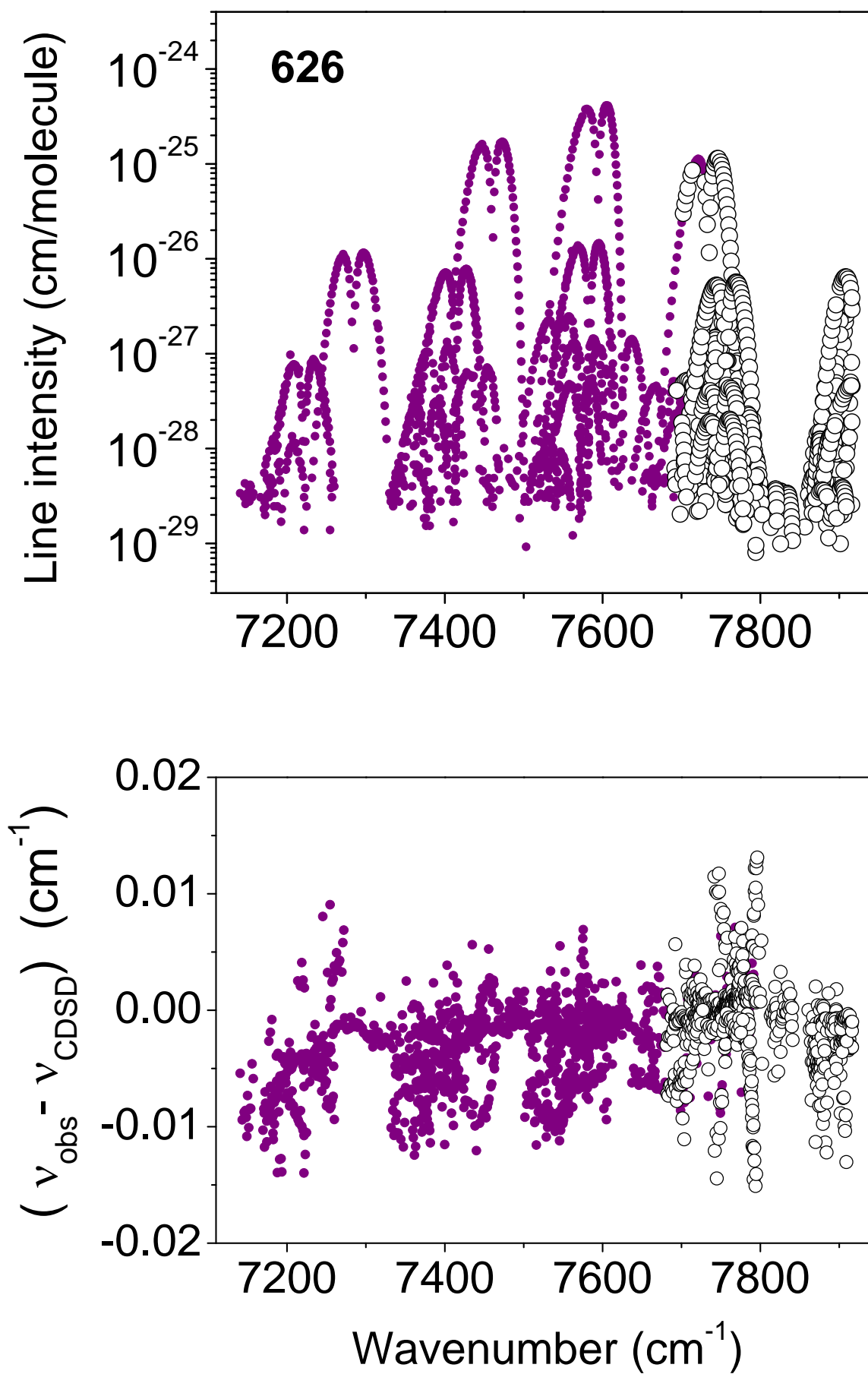
Parameter <sup>a)</sup>	$\Delta V_1$	$\Delta V_2$	$\Delta V_3$	$\Delta \ell_2$	Value	Order
$^{16}\text{O}^{12}\text{C}^{18}\text{O}$ $\Delta P=10$ series						
$M$	2	0	2	0	-0.19377(94)	$10^{-4}$
$M$	1	2	2	0	0.198(12)	$10^{-5}$
$^{12}\text{C}^{16}\text{O}_2$ $\Delta P=11$ series						
$M$	4	0	1	0	0.15863(11)	$10^{-4}$
$\kappa$	4	0	1	0	0.371(69)	$10^{-2}$
$b_J$	4	0	1	0	0.405(17)	$10^{-3}$
$M$	3	2	1	0	-0.13134(53)	$10^{-5}$
$M$	2	4	1	0	0.649(18)	$10^{-7}$
$M$	1	6	1	0	-0.197(41)	$10^{-8}$
$M$	1	0	3	0	0.74913(17)	$10^{-4}$
$M$	0	2	3	0	-0.2071(85)	$10^{-5}$
$M$	2	1	2	1	-0.26158(45)	$10^{-5}$
$b_J$	2	1	2	1	0.38321(96)	$10^{-1}$
$M$	1	3	2	1	0.1686(25)	$10^{-6}$
$b_J$	1	3	2	1	0.8196(83)	$10^{-1}$
$M$	3	-1	2	1	-0.1187(98)	$10^{-6}$
$M$	5	1	0	1	0.108(11)	$10^{-7}$
$b_J$	5	1	0	1	0.1808(40)	

<sup>a)</sup> The parameters  $M$  are given in *Debye* while the  $b_J$  parameters are dimensionless.

Only relative signs of the  $M$  parameters within a given series of transitions are determined.

<sup>b)</sup> The numbers in parentheses correspond to one standard deviation in units of the last quoted digit.

Fig. 1



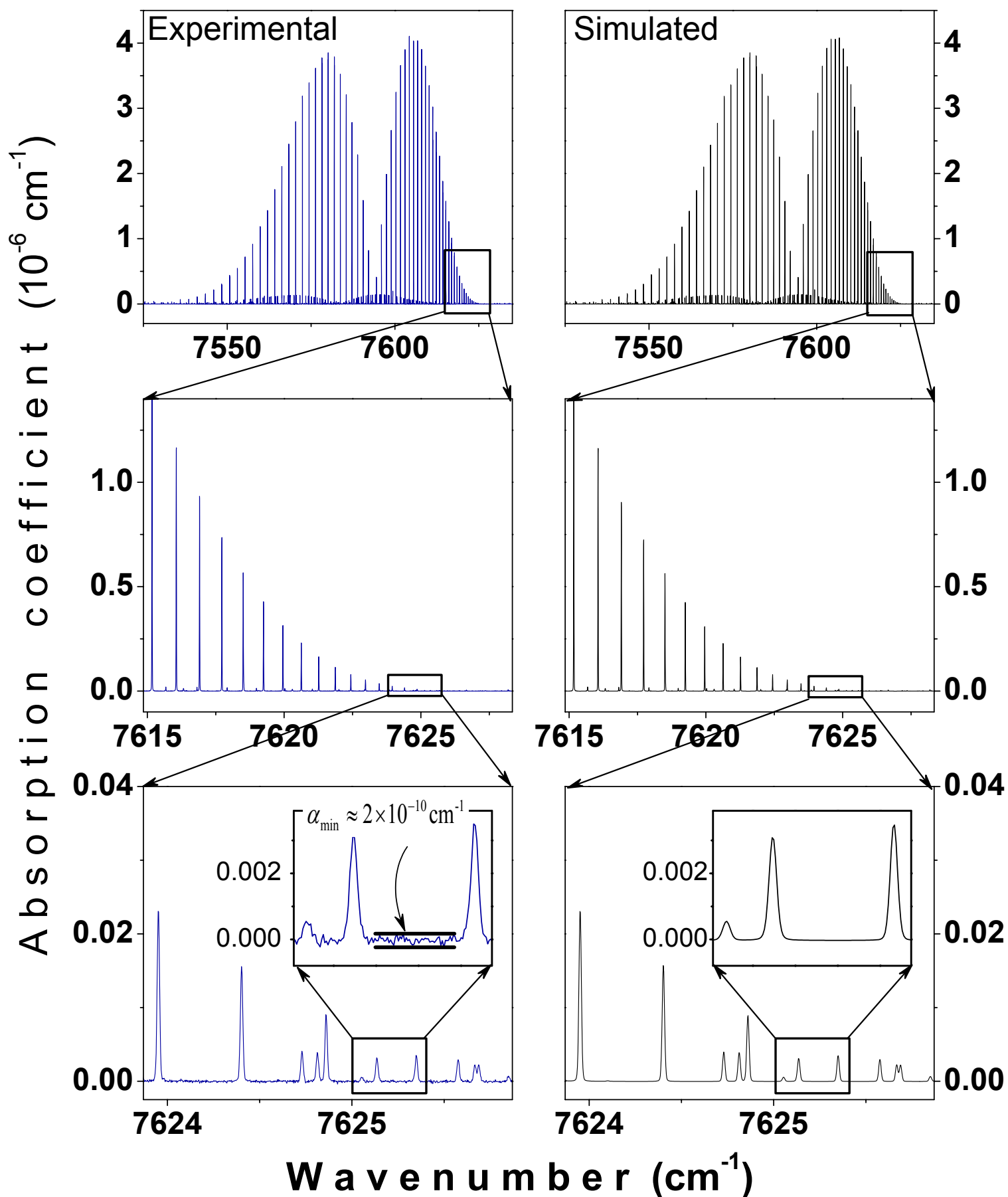
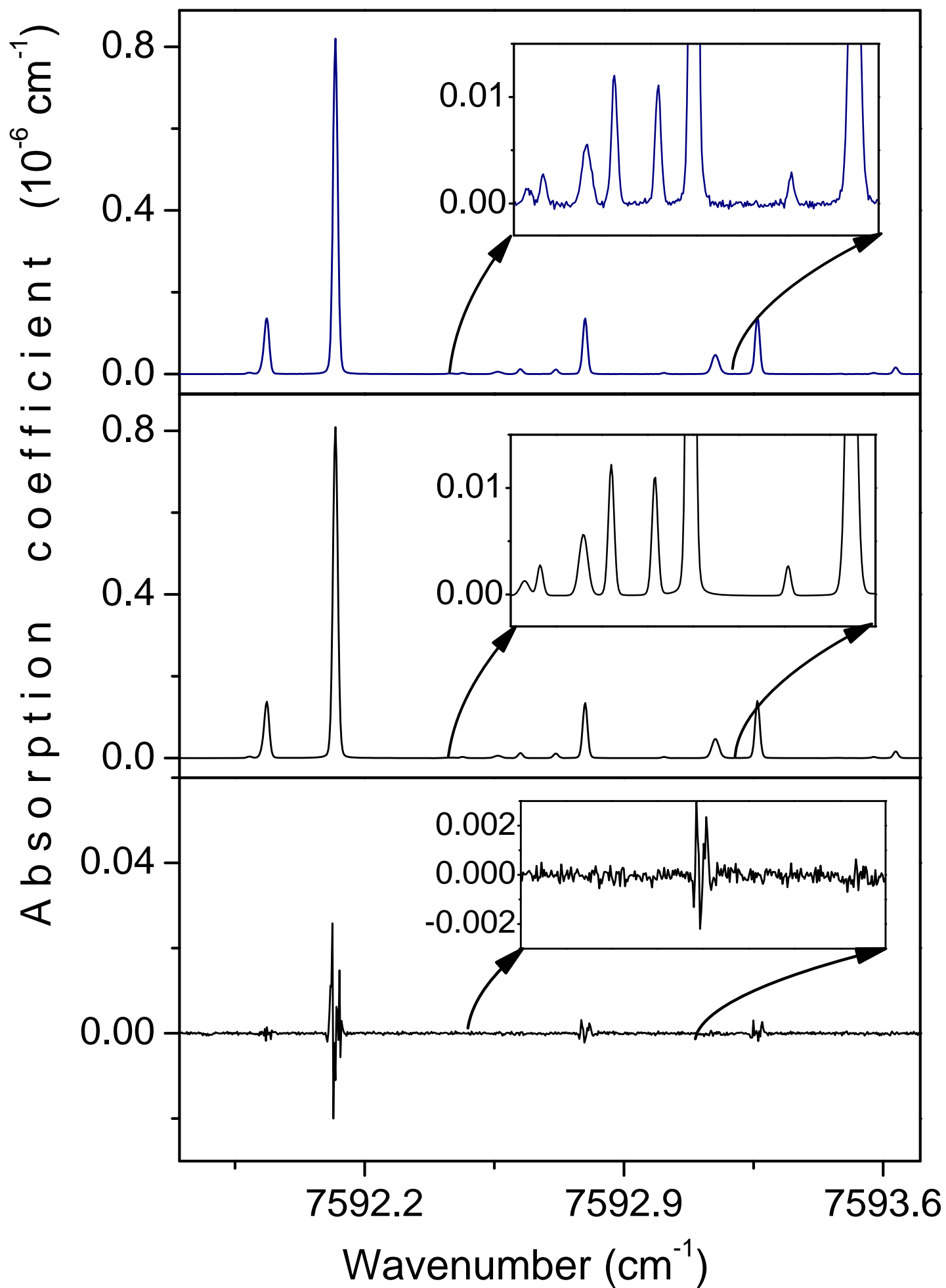


Fig. 3



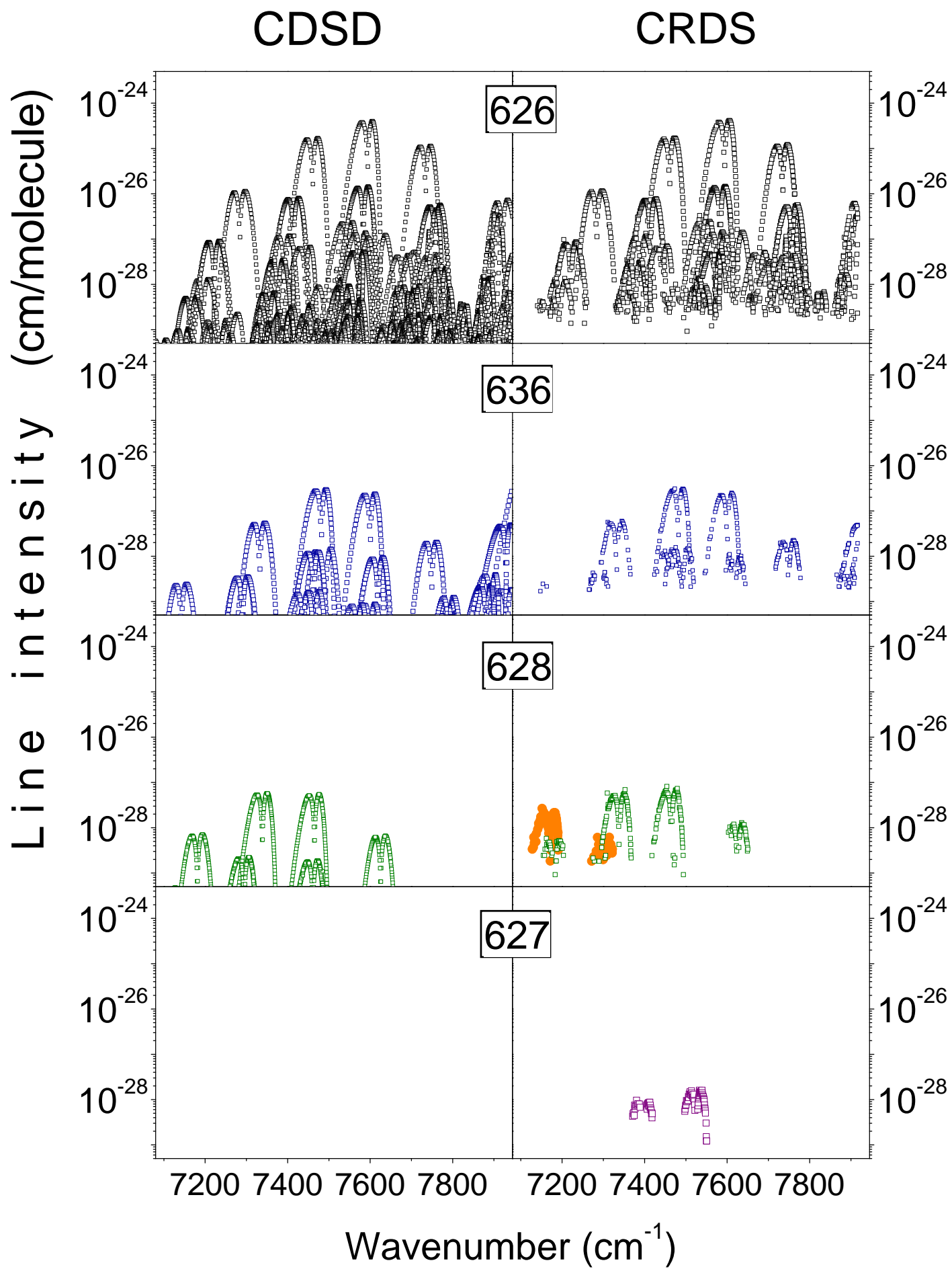


Fig. 5

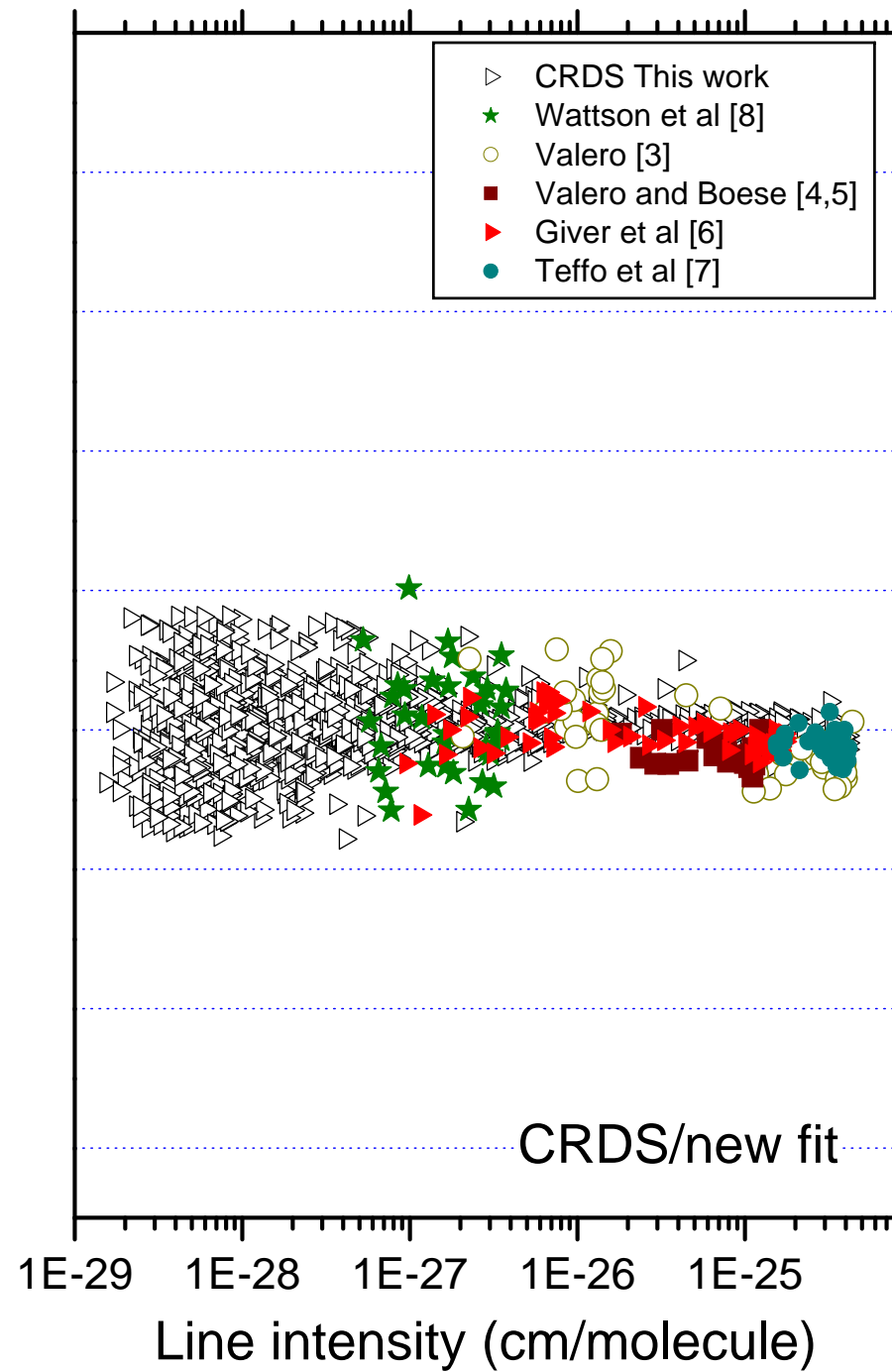
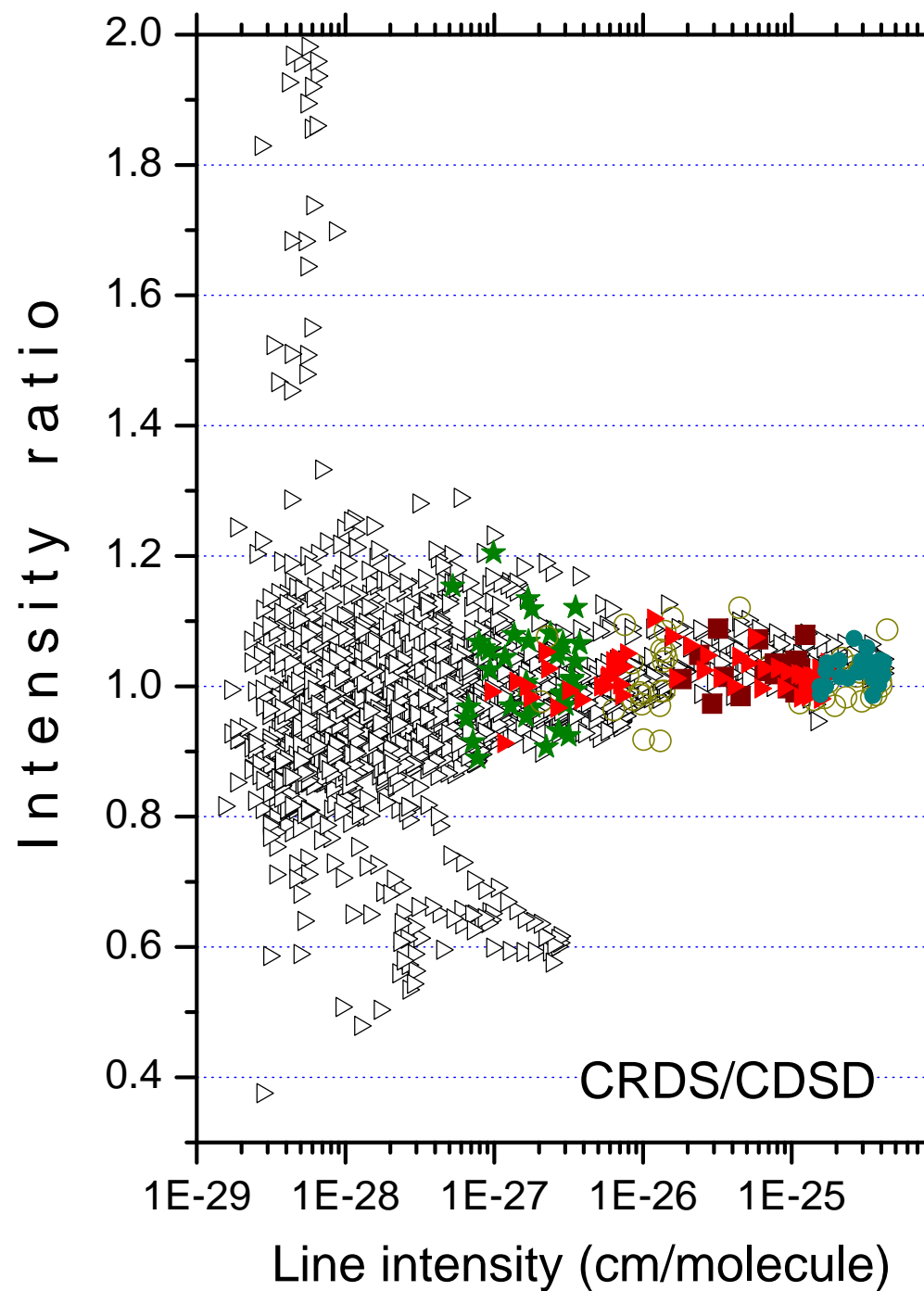
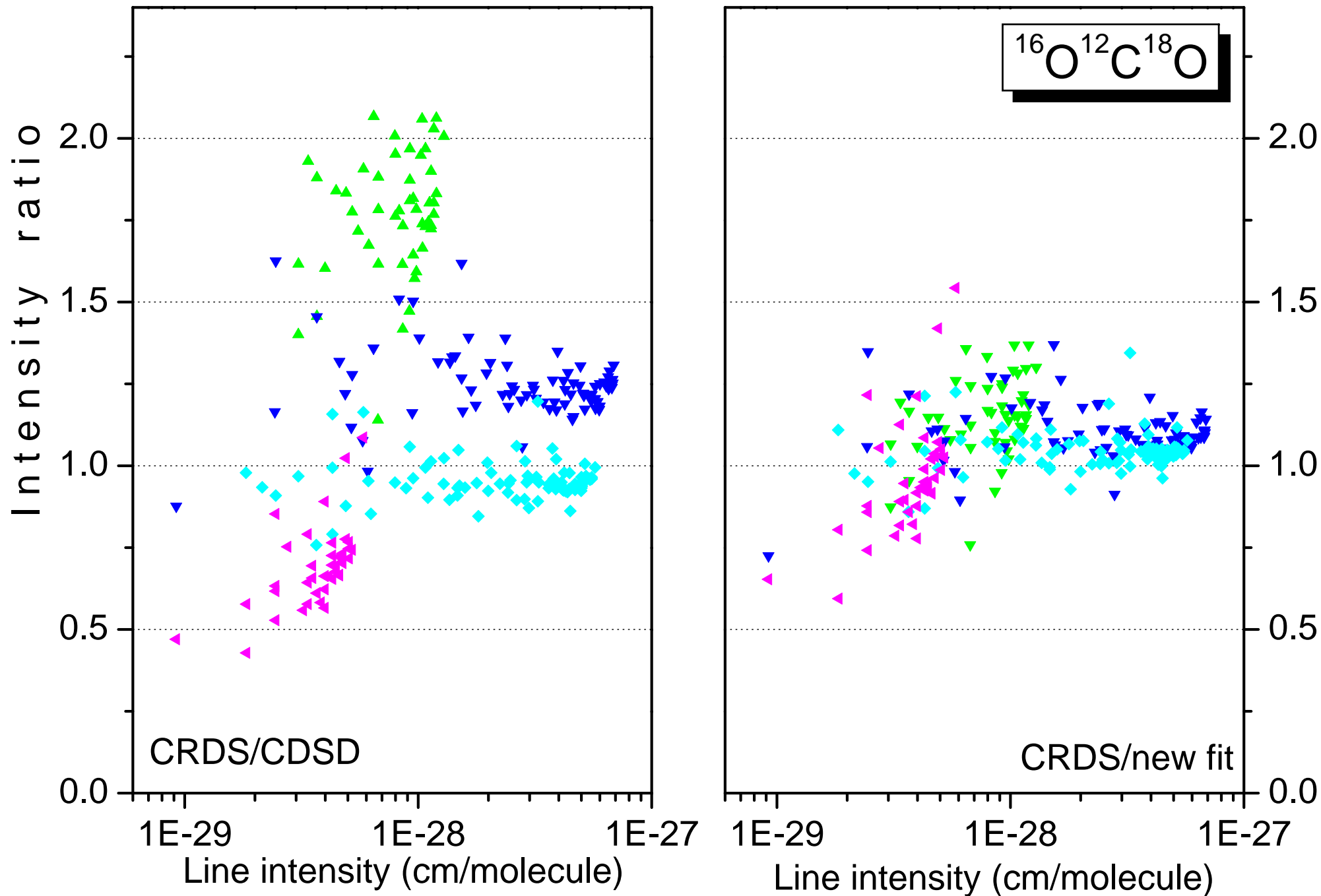


Fig. 6



e-component, for online publication only

[Click here to download e-component, for online publication only: CRDS linelist of natural CO2\\_7123-7917 cm-1 .txt](#)

**e-component, for online publication only**

**[Click here to download e-component, for online publication only: band by band\\_parameters.doc](#)**

e-component, for online publication only

[Click here to download e-component, for online publication only: 626\\_band by band fit\\_7123-7917 cm-1.txt](#)

**e-component, for online publication only**

**[Click here to download e-component, for online publication only: 627\\_band by band fit\\_7123-7917 cm-1..txt](#)**

**e-component, for online publication only**

**[Click here to download e-component, for online publication only: 628\\_band by band fit\\_7123-7917 cm-1..txt](#)**